

Two-way Relay Selection for Millimeter Wave Networks

Khagendra Belbase, Chintha Tellambura, *Fellow, IEEE*, and Hai Jiang, *Senior Member, IEEE*

Abstract—In this letter, we investigate the potential benefits of deploying two-way amplify-and-forward relays to help bidirectional data exchange between two end users in a millimeter wave (mmWave) network. While the locations of the two end users are fixed, the locations of the potential relays are modeled as a homogeneous Poisson point process. A relay is thus selected to maximize the minimum of the two users' end-to-end signal-to-noise ratios. For this system, we derive the coverage probability and show that the considered relay selection significantly outperforms the random selection scheme in terms of coverage and spectral efficiency.

Index Terms—5G, blockage, mmWave networks, relay selection, two-way relays.

I. INTRODUCTION

Massive wireless bandwidth is needed due to unprecedented capacity and data rate demands of future 5G wireless networks and Internet of things (IoT) networks. Fortunately, huge bandwidth is available in millimeter wave (mmWave) frequencies (30-300 GHz) [1]. However, in contrast to sub-6 GHz bands, mmWave systems suffer from high propagation loss, directivity, sensitivity to blockage, and losses due to mobility. Links with line-of-sight (LOS) conditions are thus necessary, and the non-line-of-sight (NLOS) regions from transmitter may lack coverage [2]. Thus, to extend coverage, densely placed mmWave relays have been investigated [1], [3], [4]. These works analyze coverage and rate of cellular mmWave **one-way** relays, where the source nodes and relays are distributed in distinct Poisson point processes (PPPs) [4].

However, the problem with one-way relays is that bidirectional data exchange between two end users requires four time slots, which can be accomplished in two time slots by using a two-way relay [5]. Thus, two-way relaying potentially doubles spectral efficiency and has been extensively studied for conventional sub-6 GHz bands (dominant with small-scale fading) with typical issues such as channel estimation [6], [7] and performance analysis [8], [9].

However, these works [6]–[9] and many similar sub-6 GHz contributions do not directly apply to mmWave links, which are fundamentally different due to directivity, path loss, blockages, and the disparity of LOS and NLOS parameters [2]. These factors decrease coverage even for nearby nodes without the presence of relays [1]. To overcome impacts of these factors, the work in [3] proposes a directional mmWave medium access protocol to overcome the blockage, and the work in [4] demonstrates the coverage improvement in a one-way relay aided mmWave network.

Manuscript received March 29, 2017; revised August 5, 2017 and Sept 19, 2017; accepted Sept 20, 2017. The associate editor coordinating the review of this paper and approving it for publication was Dr. Christos Masouros.

The authors are with the Department of Electrical and Computer Engineering, University of Alberta, Edmonton, AB, Canada, T6G 2V4 (Email: {belbase, ct4, hai1}@ualberta.ca).

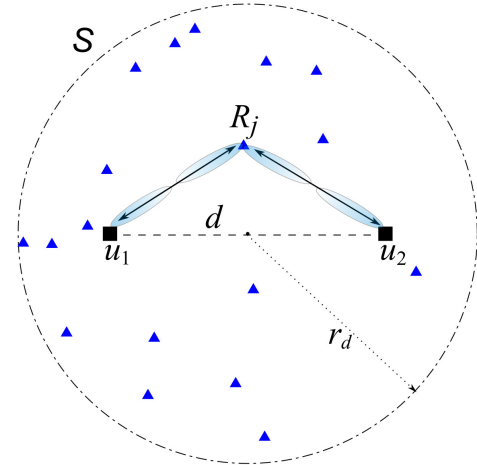


Fig. 1: Two-way relay network. Relay R_j is selected from a set of potential relay nodes (triangles).

However, to the best of our knowledge, **mmWave two-way relaying has not been studied thus far**. To fill this gap, we investigate the potential benefits of deploying two-way relays to help bidirectional data exchange between two end users. We select a relay to maximize the minimum of the two users' end-to-end signal-to-noise ratios (SNRs). We derive the coverage probability and show that the considered relay selection significantly outperforms the random selection scheme in terms of coverage and spectral efficiency.

Notations: for a random variable (r.v.) X , we use $F_X(\cdot)$ and $f_X(\cdot)$ to represent cumulative distribution function (CDF) and probability density function (PDF), respectively. \mathbb{R}^2 is the two-dimensional real plane. $\mathbb{P}(\cdot)$ and $\mathbb{E}[\cdot]$ denote probability and expectation. A log-normal r.v. $X = e^{\mu + \sigma Z}$ where Z is $\mathcal{N}(0, 1)$ is denoted by $X \sim \mathcal{LN}(\mu, \sigma^2)$, with PDF as $f_X(x) = \frac{1}{\sqrt{2\pi}\sigma} \exp\left(-\frac{(\ln x - \mu)^2}{2\sigma^2}\right)$, $x > 0$.

II. SYSTEM MODEL

A. Network Modeling

Consider two-way amplify-and-forward (AF) relaying for two end users (namely, u_1 and u_2) at a distance d (Fig. 1). The locations of potential relays in the entire \mathbb{R}^2 plane form a homogeneous PPP Φ of density λ . However, due to large path losses, we consider only nodes inside a circular disc \mathcal{S} of radius r_d ($\gg d$), centered at the mid-point of the two users. The reason is as follows. Due to heavy path loss associated with a large distance, the potential relay nodes outside of the circular disc \mathcal{S} are unlikely to be able to provide relaying service. Thus, \mathcal{S} is essentially equivalent to entire \mathbb{R}^2 .

The homogeneous PPP Φ is a collection of points $\Phi = \{z_1, z_2, \dots\}$, $z_k \in \mathbb{R}^2$. Here $z_j, j \in \{1, 2, \dots\}$ is the location of j -th relay (R_j). The total number of relays in \mathcal{S} , N , is a Poisson r.v. with mean $\lambda\pi r_d^2$. The widely used PPP

model captures the random locations of nodes and provides a tractable analysis [10]. In this letter, we assume that the potential relay nodes are deployed without significant network planning; consequently, their locations are random. This scenario is perfectly modeled by a PPP.

All the potential relay nodes use mmWave and are capable of directional beamforming. No direct link exists between u_1 and u_2 due to blockages and directivity, which necessitates the use of a relay. Also we assume that u_1 and u_2 have the same transmit power P and the j -th relay node transmits with output power Q_j . One node can serve as a central coordinator who gets all the channel state information and performs relay selection. Channel estimation can be done using pilots and additional methods [9]. The information on direction can be efficiently obtained using the existing methods [11].

B. Path Loss, Directivity and Blockage Modeling

The path loss is generally modeled by applying a linear fit to the path loss data from propagation measurements. The shadowing component is typically modeled as log-normal. We use the model in [2] which incorporates the log-normal shadowing and free-space path loss. Consequently, the total channel attenuation between two points $a, b \in \mathbb{R}^2$ is given by

$$L_l(a, b)[dB] = \beta_l + 10\alpha_l \log_{10} \|a - b\| + \mathcal{X}_l \quad (1)$$

where $\|a - b\|$ means distance between points a and b , $\mathcal{X}_l \sim \mathcal{N}(0, \sigma_l^2)$ models the deviation in fitting, and $l \in \{L, N\}$ indicates the LOS and NLOS conditions that dictate the choice of α_l , β_l and σ_l^2 . One interpretation of α_l and β_l is that α_l is the path loss exponent and β_l represents path loss at a reference point. We use this interpretation in our analysis and we write $\beta_l = 20 \log_{10} \left(\frac{\eta}{4\pi}\right) = \beta$, where η is the wavelength of the mmWave frequency.

We model the directivity as a function of azimuth angle θ where the antenna possesses the gain G_{\max} within its half power beamwidth (ϕ), and G_{\min} in all other directions [10]. In other words, for gain $G(\theta)$, we have $G(\theta) = G_{\max}$, if $|\theta| \leq \frac{\phi}{2}$, or $G(\theta) = G_{\min}$ otherwise. In our analysis, we first consider perfect beam alignment between the communicating nodes, i.e., $u_1 - R_j$ or $u_2 - R_j$, which provides the effective antenna gain, $G_{\text{eq}} = G_{\max}^2$ in a given link and derive coverage probability. The misalignment of the beams is analyzed in Section III-C.

The effect of blockages is modeled using the fixed LOS ball model [10], where two points within a distance D have a constant probability ω of being in LOS. The parameters ω and D are propagation environment dependent and obtained from geographic data [10].

C. SNR Modeling

Considering the j -th node (R_j) to be used, the SNR for the $u_k - R_j$, ($k = 1, 2$) link can be written as

$$\gamma_{u_k, R_j} = P \Gamma_{u_k, R_j} \quad (2)$$

where Γ_{u_k, R_j} incorporates the effect of path loss, blockage, beamforming gain at transmitter and receiver, and noise power at receiver, and is defined as

$$\Gamma_{u_k, R_j} \triangleq \frac{G_{\text{eq}}}{N_0} \left(\frac{\omega}{L_L(u_k, R_j)} + \frac{1 - \omega}{L_N(u_k, R_j)} \right), \quad (3)$$

where N_0 is the noise power at the receiver, and $L_l(u_k, R_j)$ is from (1). The attenuation $L_l(a, b)[dB]$ can be written in linear scale as $L_l(a, b) = 10^{(\beta_l + \mathcal{X}_l)/10} \|a - b\|^{\alpha_l}$. Using the linear scale notations, (3) can be rewritten as

$$\Gamma_{u_k, R_j} = \underbrace{\mathcal{K} \omega e^{-\mathcal{X}_L} r_{k,j}^{-\alpha_L}}_{\mathcal{Y}} + \underbrace{\mathcal{K} (1 - \omega) e^{-\mathcal{X}_N} r_{k,j}^{-\alpha_N}}_{\mathcal{Z}}, \quad (4)$$

where $\mathcal{K} = \frac{10^{-\beta/10} \xi G_{\text{eq}}}{N_0}$, $\xi = \frac{\ln(10)}{10}$ is a constant used to convert dB to natural logarithm, $r_{k,j}$ is the distance between u_k ($k = 1, 2$) and relay R_j , and $e^{-\mathcal{X}_L} \sim \mathcal{LN}(0, \sigma_L^2)$ and $e^{-\mathcal{X}_N} \sim \mathcal{LN}(0, \sigma_N^2)$ are two independent log-normal r.v.s for LOS and NLOS links, respectively. Using the scaling property of log-normal r.v.s, the two summands in (4) satisfy $\mathcal{Y} \sim \mathcal{LN}(\mathcal{K} \omega r_{k,j}^{-\alpha_L}, \sigma_L^2)$ and $\mathcal{Z} \sim \mathcal{LN}(\mathcal{K} (1 - \omega) r_{k,j}^{-\alpha_N}, \sigma_N^2)$. Then, the total sum Γ_{u_k, R_j} can be approximated by a log-normal r.v. using the Fenton-Wilkinson method [12].

Using the channel reciprocity, the relay-to-user link ($R_j - u_k$, $k \in \{1, 2\}$) SNRs can be written as

$$\gamma_{R_j, u_k} = Q_j \Gamma_{u_k, R_j}.$$

The end-to-end receive SNR γ_{k, R_j} of u_k , $k \in \{1, 2\}$ when relay R_j ($j = 1, 2, \dots, N$) is used can be written as [8, eq. (2)]

$$\gamma_{k, R_j} = \frac{P Q_j \Gamma_{u_k, R_j} \Gamma_{u_{\bar{k}}, R_j}}{1 + (P + Q_j) \Gamma_{u_k, R_j} + P \Gamma_{u_{\bar{k}}, R_j}} \quad (5)$$

where we denote $\{\bar{k}\} \triangleq \{1, 2\} \setminus \{k\}$.

III. RELAY SELECTION

A relay is selected from Φ to maximize the reliability of both users u_1 and u_2 , i.e., maximize the minimum of the two users' end-to-end SNRs. The selection criterion may thus be stated as

$$\mathcal{R} = \arg \max_j \min\{\gamma_{1, R_j}, \gamma_{2, R_j}\}, \quad (6)$$

where γ_{1, R_j} and γ_{2, R_j} are the end-to-end SNRs given in (5).

A. Coverage Probability

With relay selection (6), *coverage* is defined as the probability that the minimum end-to-end SNR of the two users is above a predefined threshold γ_{th} . Since the potential relays are located randomly in the disc \mathcal{S} with radius $r_d \gg d$ with a PPP of density λ , the number of nodes in \mathcal{S} , N , is a Poisson r.v. with mean $\lambda |\mathcal{S}|$, where $|\mathcal{S}| = \pi r_d^2$ is the area of \mathcal{S} . For a realization of PPP with N nodes, SNR with relay selection is given by

$$\gamma_{\mathcal{R}} = \begin{cases} \max\{\gamma_1, \gamma_2, \dots, \gamma_N\}, & \text{if } N \neq 0 \\ 0, & \text{if } N = 0 \end{cases} \quad (7)$$

where $\gamma_{\mathcal{R}}$ is the equivalent end-to-end SNR of selected relay \mathcal{R} , and $\gamma_j = \min\{\gamma_{1, R_j}, \gamma_{2, R_j}\}$. Subsequently, we will denote γ_j by γ_z since it represents an arbitrary node in Φ . From the properties of PPP, given $N = k > 0$, the location z is uniformly distributed in \mathcal{S} and γ_z 's are independent.

Thus, with relay selection (6), the coverage probability can be evaluated as

$$\begin{aligned}
P_{\text{cov}} &= \mathbb{P}(\gamma_{\mathcal{R}} \geq \gamma_{th}) = 1 - \mathbb{P}\left(\max_{z \in \Phi} \gamma_z \leq \gamma_{th}\right) \\
&\stackrel{(a)}{=} 1 - \mathbb{E}_{\Phi} \left[\prod_{z \in \Phi} \mathbb{P}(\gamma_z \leq \gamma_{th}) \right] \\
&\stackrel{(b)}{=} 1 - \sum_{k=1}^{\infty} \mathbb{P}(N = k) \mathbb{E}_z \left[\prod_{z \in \Phi} F_{\gamma_z}(\gamma_{th} | N = k) \right] \\
&\stackrel{(c)}{=} 1 - \sum_{k=1}^{\infty} \frac{e^{-\lambda|\mathcal{S}|} (\lambda|\mathcal{S}|)^k}{k!} \mathbb{E}_z \left[F_{\gamma_z}(\gamma_{th}) \right]^k \\
&= 1 - e^{-\lambda|\mathcal{S}|} \sum_{k=1}^{\infty} \frac{(\lambda|\mathcal{S}|)^k}{k!} \nu^k \\
&= 1 - e^{-\lambda|\mathcal{S}|} (e^{\lambda|\mathcal{S}|\nu} - 1) \tag{8}
\end{aligned}$$

where (a) follows from independence of individual γ_z 's, in (b) the sum starts from $k = 1$ since we assume $N = k > 0$, (c) uses the probability for Poisson distribution, and ν is the outage probability of a randomly located relay uniformly distributed over \mathcal{S} and is given by [13]

$$\nu = \mathbb{E}_z \left[F_{\gamma_z}(\gamma_{th}) \right] = \frac{1}{|\mathcal{S}|} \int_0^{2\pi} \int_0^{r_d} F_{\gamma_z}(\gamma_{th}) r dr d\theta \tag{9}$$

where given z , $F_{\gamma_z}(\gamma_{th})$ is the conditional CDF of end-to-end SNR γ_z . The value of ν is then obtained numerically by averaging $F_{\gamma_z}(\gamma_{th})$ over Φ .

B. CDF expression of γ_z

Expression of $F_{\gamma_z}(\gamma_{th})$ is needed to compute the outage probability ν in (9). To derive $F_{\gamma_z}(\gamma_{th})$, we condition the location of R_j to be z . Specifically, we first derive the conditional CDF $F_{\gamma_z}(\gamma_{th})$ of minimum end-to-end SNR $\gamma_j = \min\{\gamma_{1,R_j}, \gamma_{2,R_j}\}$ conditioned on the location z , and then compute its expected value as in (9). For simplicity, the conditional notation is omitted.

Let $X \triangleq \Gamma_{u_1, R_j}$ and $Y \triangleq \Gamma_{u_2, R_j}$, where $X \sim \mathcal{LN}(\mu_x, \sigma_x^2)$ and $Y \sim \mathcal{LN}(\mu_y, \sigma_y^2)$. Now the CDF of $\min\{\gamma_{1,R_j}, \gamma_{2,R_j}\}$ can be written as

$$\begin{aligned}
F_{\gamma}(\gamma_{th}) &= 1 - \mathbb{P}(\min\{\gamma_{1,R_j}, \gamma_{2,R_j}\} > \gamma_{th}) \\
&= 1 - \underbrace{\mathbb{P}(\gamma_{2,R_j} > \gamma_{th}, X < Y)}_{Pr_1} - \underbrace{\mathbb{P}(\gamma_{1,R_j} > \gamma_{th}, X > Y)}_{Pr_2}. \tag{10}
\end{aligned}$$

Here Pr_1 is given by

$$\begin{aligned}
Pr_1 &= \mathbb{P}\left(\frac{PQ_jXY}{PX + (P+Q_j)Y + 1} > \gamma_{th}, X < Y\right) \\
&= \int_a^{\infty} \mathbb{P}\left(y > \max\left\{x, \frac{(1+Px)\gamma_{th}}{PQ_jx - (P+Q_j)\gamma_{th}}\right\}\right) f_X(x) dx \\
&= \int_a^b \mathbb{P}\left(y > \frac{(1+Px)\gamma_{th}}{PQ_jx - (P+Q_j)\gamma_{th}}\right) f_X(x) dx \\
&\quad + \int_b^{\infty} \mathbb{P}(y > x) f_X(x) dx \\
&= \int_a^b \int_{c_1}^{\infty} f_Y(y) f_X(x) dy dx + \int_b^{\infty} \int_x^{\infty} f_Y(y) f_X(x) dy dx, \tag{11}
\end{aligned}$$

where $c_1 = \frac{(1+Px)\gamma_{th}}{PQ_jx - (P+Q_j)\gamma_{th}}$, $a = \frac{P+Q_j}{PQ_j} \gamma_{th}$ and $b = \frac{(2P+Q_j)\gamma_{th} + \sqrt{(2P+Q_j)^2\gamma_{th}^2 + 4PQ_j\gamma_{th}}}{2PQ_j}$. Similarly, Pr_2 can be derived as

$$\begin{aligned}
Pr_2 &= \mathbb{P}\left(\frac{PQ_jXY}{(P+Q_j)X + PY + 1} > \gamma_{th}, X > Y\right) \\
&= \int_b^{\infty} \mathbb{P}\left(y > \frac{(1+(P+Q_j)x)\gamma_{th}}{PQ_jx - P\gamma_{th}}, y < x\right) f_X(x) dx \\
&= \int_b^{\infty} \int_{c_2}^x f_Y(y) f_X(x) dy dx \tag{12}
\end{aligned}$$

where $c_2 = \frac{(1+(P+Q_j)x)\gamma_{th}}{PQ_jx - P\gamma_{th}}$. By substituting (11) and (12) in (10) and with some mathematical manipulation, we get

$$\begin{aligned}
F_{\gamma}(\gamma_{th}) &= 1 - \int_a^b \int_{c_1}^{\infty} f_Y(y) dy f_X(x) dx - \int_b^{\infty} \int_{c_2}^{\infty} f_Y(y) dy f_X(x) dx \\
&= 1 - \int_a^b Q\left(\frac{\ln c_1 - \mu_y}{\sigma_y}\right) \frac{1}{\sqrt{2\pi x \sigma_x}} \exp\left(-\frac{(\ln x - \mu_x)^2}{2\sigma_x^2}\right) dx \\
&\quad - \int_b^{\infty} Q\left(\frac{\ln c_2 - \mu_y}{\sigma_y}\right) \frac{1}{\sqrt{2\pi x \sigma_x}} \exp\left(-\frac{(\ln x - \mu_x)^2}{2\sigma_x^2}\right) dx. \tag{13}
\end{aligned}$$

Now by substituting $\frac{\ln x - \mu_x}{\sqrt{2\sigma_x}} = u$ in (13), we get

$$\begin{aligned}
F_{\gamma}(\gamma_{th}) &= 1 - \frac{1}{\sqrt{\pi}} \int_{a'}^{b'} Q\left(\frac{\ln c'_1 - \mu_y}{\sqrt{2}\sigma_y}\right) e^{-u^2} du \\
&\quad - \frac{1}{\sqrt{\pi}} \int_{b'}^{\infty} Q\left(\frac{\ln c'_2 - \mu_y}{\sqrt{2}\sigma_y}\right) e^{-u^2} du \tag{14}
\end{aligned}$$

where $a' = \frac{\ln a - \mu_x}{\sqrt{2}\sigma_x}$, $b' = \frac{\ln b - \mu_x}{\sqrt{2}\sigma_x}$, $Q(\cdot)$ is the upper tail probability of the standard Gaussian distribution, and c'_1 and c'_2 are obtained by substituting $x = e^{(\mu_x + \sqrt{2}\sigma_x u)}$ in c_1 and c_2 , respectively. The integrals in (14) can now be calculated with one sided Gauss-Hermite Quadrature rule [14].

C. Coverage Probability with Beamsteering Errors

In Section II-B, coverage (8) is derived for no beamsteering errors. Next we consider the case with beam alignment error. We use the analytical method given in [15], as follows. Assume the beamsteering error of either $u_1 - R_j$ or $u_2 - R_j$ link is a Gaussian r.v. $\varepsilon \sim \mathcal{N}(0, \sigma_{\mathbb{E}}^2)$. Then its absolute value $|\varepsilon|$ follows a half normal distribution, and its CDF is $F_{|\varepsilon|}(x) = \text{erf}(x/(\sqrt{2}\sigma_{\mathbb{E}}))$, in which $\text{erf}(\cdot)$ is the Gauss error function. The effective antenna gain G_{eq} for either $u_1 - R_j$ or $u_2 - R_j$ link has the following PDF

$$\begin{aligned}
f_{G_{\text{eq}}}(g) &= F_{|\varepsilon|}\left(\frac{\phi}{2}\right)^2 \delta_{(g-G_{\text{max}}^2)} + 2F_{|\varepsilon|}\left(\frac{\phi}{2}\right) \left(1 - F_{|\varepsilon|}\left(\frac{\phi}{2}\right)\right) \\
&\quad \times \delta_{(g-G_{\text{max}}G_{\text{min}})} + \left(1 - F_{|\varepsilon|}\left(\frac{\phi}{2}\right)\right)^2 \delta_{(g-G_{\text{min}}^2)},
\end{aligned}$$

in which $\delta_{(\cdot)}$ represents the Kronecker delta function. Accordingly, the overall coverage probability P_{cov} can be calculated as:

$$\begin{aligned}
P_{\text{cov}} &= \int_0^{\infty} P_{\text{cov}}(g) f_{G_{\text{eq}}}(g) dg \\
&= F_{|\varepsilon|}(\phi/2)^2 P_{\text{cov}}(G_{\text{max}}^2) + 2F_{|\varepsilon|}(\phi/2) (1 - F_{|\varepsilon|}(\phi/2)) \\
&\quad \times P_{\text{cov}}(G_{\text{max}}G_{\text{min}}) + (1 - F_{|\varepsilon|}(\phi/2))^2 P_{\text{cov}}(G_{\text{min}}^2) \tag{15}
\end{aligned}$$

where $P_{\text{cov}}(g)$ means the coverage probability as a function of the gain.

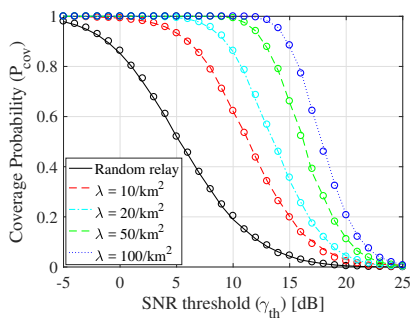


Fig. 2: Coverage vs. threshold for several relay densities.

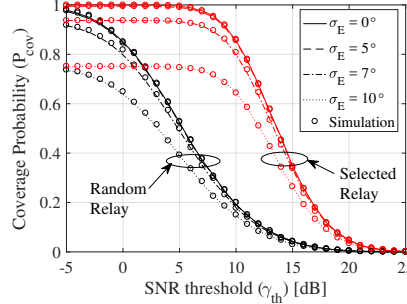


Fig. 3: Coverage vs. SNR threshold for different beamsteering errors (σ_E), when $\phi = 30^\circ$ and $\lambda = 20/\text{km}^2$.

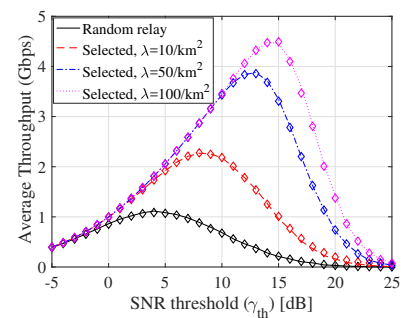


Fig. 4: Average user throughput for different SNR thresholds.

IV. NUMERICAL RESULTS AND SIMULATIONS

In this section, our analytical results are verified with Monte-Carlo simulation (10^5 independent realizations of PPP). We consider a carrier frequency of 73 GHz with bandwidth $W = 1$ GHz, and all nodes have directional antennas with gains $G_{\max} = 18\text{dB}$ and $G_{\min} = -10\text{dB}$. We set $\alpha_L = 2$, $\alpha_N = 3.3$, $\sigma_L = 5.2$ dB and $\sigma_N = 7.6$ dB [10]. The transmit power of 30 dBm is used for all the nodes, i.e., u_1 and u_2 and relays. In the figures, the curves represent analysis, and the markers are for simulated results. Clearly, analytical results match exactly with simulations, verifying the correctness of our analysis.

Fig. 2 plots coverage probability versus the SNR threshold for the selected relay in (6) and that of a random relay, for various node densities. We can observe that as the node density increases from $10/\text{km}^2$ to $100/\text{km}^2$, the coverage improves from 20% to 90% for a 15 dB threshold. In Fig. 3, we plot the effect of beamsteering error on coverage probability. We can observe that for small beamsteering error (σ_E) of up to 5 degrees, the performance is very close to that of perfect beam alignment case. However, when σ_E exceeds 7 degrees, the coverage probability starts to decrease for both the randomly picked relay and the selected relay.

Fig. 4 shows the effect of relay density in average user throughput, which is calculated as $C = WP_{\text{cov}} \log_2(1 + \gamma_{th})$. The achieved throughput with a random relay is always less than that of the optimally selected relay per (6), and increasing the relay density increases the throughput of the system.

V. CONCLUSIONS

We study the two-way AF relay selection in a mmWave wireless network. The challenge is to improve the bidirectional communication between two fixed end users. The locations of potential relay nodes are modeled as a homogeneous PPP. The best relay is selected to maximize the minimum of the two users' end-to-end SNR. We derive the exact CDF of the minimum end-to-end SNR with a random relay, and use it to get the coverage probability of relay selection (6). It is found that relay selection (6) provides significantly better coverage and spectral efficiency compared to the random selection scheme. Increasing the node density also improves coverage due to spatial diversity. Overall, two-way relay selection in mmWave networks appears to offer significant benefits. Future works may consider other relay selection criteria.

REFERENCES

- [1] S. Rangan, T. S. Rappaport, and E. Erkip, "Millimeter wave cellular wireless networks: Potentials and challenges," *Proc. IEEE*, vol. 102, no. 3, pp. 366–385, Mar. 2014.
- [2] M. R. Akdeniz, Y. Liu, M. K. Samimi, S. Sun, S. Rangan, T. S. Rappaport, and E. Erkip, "Millimeter wave channel modeling and cellular capacity evaluation," *IEEE J. Sel. Areas Commun.*, vol. 32, no. 6, pp. 1164–1179, June 2014.
- [3] S. Singh, F. Ziliotto, U. Madhow, E. Belding, and M. Rodwell, "Blockage and directivity in 60 GHz wireless personal area networks: From cross-layer model to multihop MAC design," *IEEE J. Sel. Areas Commun.*, vol. 27, no. 8, pp. 1400–1413, Oct. 2009.
- [4] S. Biswas, S. Vuppala, J. Xue, and T. Ratnarajah, "On the performance of relay aided millimeter wave networks," *IEEE J. Sel. Topics Signal Process.*, vol. 10, no. 3, pp. 576–588, Apr. 2016.
- [5] C. E. Shannon *et al.*, "Two-way communication channels," in *Proc. 4th Berkeley Symp. Math. Stat. Prob.*, vol. 1. Citeseer, 1961, pp. 611–644.
- [6] G. Wang, F. Gao, W. Chen, and C. Tellambura, "Channel estimation and training design for two-way relay networks in time-selective fading environments," *IEEE Trans. Wireless Commun.*, vol. 10, no. 8, pp. 2681–2691, Aug. 2011.
- [7] G. Wang, F. Gao, Y.-C. Wu, and C. Tellambura, "Joint CFO and channel estimation for OFDM-based two-way relay networks," *IEEE Trans. Wireless Commun.*, vol. 10, no. 2, pp. 456–465, Feb. 2011.
- [8] Y. Jing, "A relay selection scheme for two-way amplify-and-forward relay networks," in *Proc. 2009 Int. Conf. on Wireless Commun. Signal Process.*, (WCSP), Nov. 2009, pp. 1–5.
- [9] S. Atapattu, Y. Jing, H. Jiang, and C. Tellambura, "Relay selection schemes and performance analysis approximations for two-way networks," *IEEE Trans. Commun.*, vol. 61, no. 3, pp. 987–998, Mar. 2013.
- [10] S. Singh, M. N. Kulkarni, A. Ghosh, and J. G. Andrews, "Tractable model for rate in self-backhauled millimeter wave cellular networks," *IEEE J. Sel. Areas Commun.*, vol. 33, no. 10, pp. 2196–2211, Oct. 2015.
- [11] J. Wang, "Beam codebook based beamforming protocol for multi-gbps millimeter-wave wpan systems," *IEEE J. Sel. Areas Commun.*, vol. 27, no. 8, pp. 1390–1399, Oct. 2009.
- [12] L. Fenton, "The sum of log-normal probability distributions in scatter transmission systems," *IRE Trans. Commun.*, vol. 8, no. 1, pp. 57–67, Mar. 1960.
- [13] M. Haenggi, *Stochastic geometry for wireless networks*. Cambridge University Press, 2012.
- [14] N. Steen, G. Byrne, and E. Gelbard, "Gaussian quadratures for the integrals $\int_0^\infty \exp(-x^2)f(x)dx$ and $\int_0^b \exp(-x^2)f(x)dx$," *Mathematics of Computation*, vol. 23, no. 107, pp. 661–671, May 1969.
- [15] E. Turgut and M. C. Gursoy, "Coverage in heterogeneous downlink millimeter wave cellular networks," *IEEE Trans. Commun.*, 2017, doi: 10.1109/TCOMM.2017.2705692, IEEE.